EFFECT OF AEROELASTIC-PROPULSIVE INTERACTIONS ON FLIGHT DYNAMICS OF A HYPERSONIC VEHICLE

David L. Raney and John D. McMinn
NASA Langley Research Center
Hampton, VA 23681

Anthony S. Pototzky
Lockheed Engineering Sciences Co.

Christine L. Wooley
University of Cincinnati

NASA LaRC Workshop on Guidance, Navigation, Controls, and Dynamics for Atmospheric Flight
March 19, 1993

Outline

Motivation and Objectives

Model Description

Propulsion Sensitivities

Impact on Flight Dynamics

Concluding Remarks

Motivation and Objectives

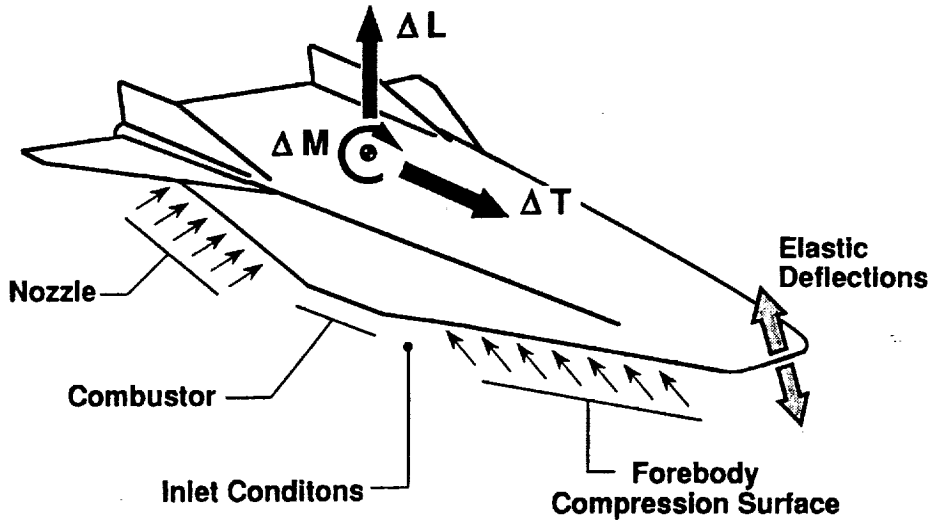

- **Assess magnitudes of propulsive force and moment perturbations**
- **Examine impact on longitudinal flight dynamics**

MOTIVATION AND OBJECTIVES

The desire to achieve orbit-on-demand access to space with rapid turn-around capability and aircraft-like processing operations has given rise to numerous hypersonic aerospace plane design concepts which would take off horizontally from a conventional runway and employ air-breathing scramjet propulsion systems for acceleration to orbital speeds. Most of these air-breathing hypersonic vehicle concepts incorporate an elongated fuselage forebody to act as the aerodynamic compression surface for a scramjet combustor module. This type of airframe-integrated scramjet propulsion system tends to be highly sensitive to inlet conditions and angle-of-attack perturbations. Furthermore, the basic configuration of the fuselage, with its elongated and tapered forebody, produces relatively low frequency elastic modes which will cause perturbations in the combustor inlet conditions due to the oscillation of the forebody compression surface. The flexibility of the forebody compression surface, together with sensitivity of scramjet propulsion systems to inlet conditions, creates the potential for an unprecedented form of aeroelastic-propulsive interaction in which deflections of the vehicle fuselage give rise to propulsion transients, producing force and moment variations that may adversely impact the longitudinal flight dynamics and/or excite the elastic modes. These propulsive force and moment variations may have an appreciable impact on the performance, guidance, and control of a hypersonic aerospace plane. The objectives of this research are (1) to quantify the magnitudes of propulsive force and moment perturbations resulting from elastic deformation of a representative hypersonic vehicle, and (2) to assess the potential impact of these perturbations on the vehicle's longitudinal flight dynamics.

Vehicle Geometry

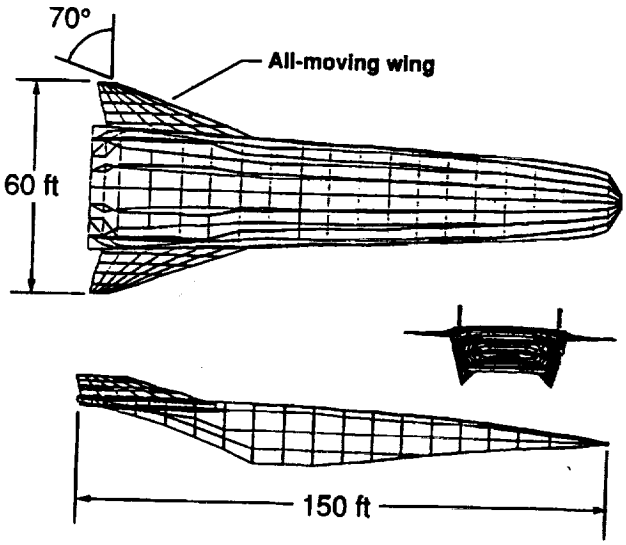

VEHICLE GEOMETRY

A three-view finite element representation of the vehicle concept used in this modeling effort is shown in the figure. It is a hypersonic lifting body with underslung engine nacelles, very similar in configuration to the proposed X-30 research vehicle. The vehicle length is 150 ft. The wingspan is 60 ft, with a wing sweep angle of 70 degrees. Vertical fins project from the upper surface of the aft fuselage near the wing root. The configuration is equipped with all-moving wing control effectors. At hypersonic speeds, the lower surface of the elongated fuselage forebody acts as a compression wedge for the scramjet combustor unit, and the lower surface of the aft portion of the vehicle acts as a nozzle. The weight of the vehicle used in this study was 300,000 lb. The configuration was analyzed at two hypersonic flight conditions: Mach 6 at 75,000 feet and Mach 10 at 95,000 feet, representing two points along a typical ascent trajectory. The dynamic pressures at these two flight conditions are 1,840 psf and 2,010 psf, respectively.

Aeroelastic Model

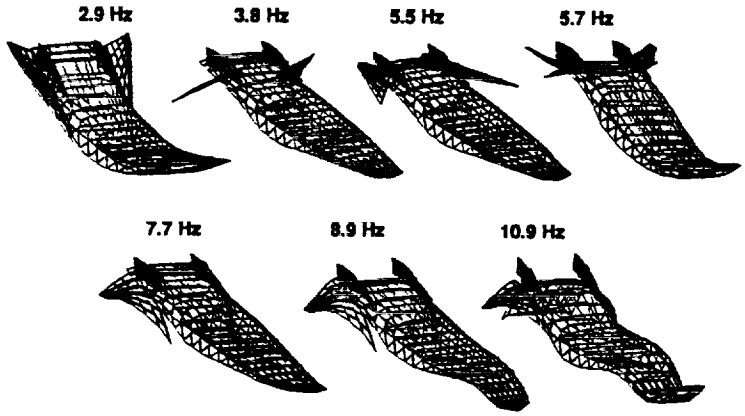

- **2 Rigid Body Modes, 7 Elastic Modes, 3rd Order Actuator**
- **General form of model:** $\dot{x} = [A]\,x + [B]\,u$

$$y = [C]\,x$$

$$x = \begin{Bmatrix} \text{rigid body states} \\ \text{elastic states} \\ \text{actuator states} \end{Bmatrix} \qquad y = \begin{Bmatrix} \text{fuselage deflections} \\ \text{angle of attack} \end{Bmatrix}$$

$$u = \{\text{control command}\}$$

AEROELASTIC MODEL

The aeroelastic state-space model used in this study is a longitudinal approximation. The model includes seven symmetric bending modes and two rigid body modes. The rigid body degrees of freedom are pitch and vertical translation (plunge). No translational degree of freedom along the vehicle's longitudinal axis is included. The general form of this aeroelastic model is shown in equations (1) and (2).

$$\dot{x} = [A]\,x + [B]\,u \qquad (1)$$
$$y = [C]\,x \qquad (2)$$

The state vector, x, contains a total of 21 elements; two for each of the nine second-order dynamic modes, and three states for an actuator model associated with the all-moving wing. The input vector, u, corresponds to the all-moving wing control command. The output vector, y, includes the rigid body angle of attack and pitch rate, as well as displacements, slopes, and accelerations at various locations throughout the fuselage and wing.

Numerical values for the matrices [A], [B], and [C] appearing in equations (1) and (2) were generated using the Interaction of Structures, Aerodynamics, and Controls code, ISAC. Second-order piston theory was used to model the unsteady aerodynamic effects at the two selected hypersonic flight conditions. The shapes and in-vacuo frequencies of the seven elastic modes are shown in the figure. Mode shapes which strongly impact the fuselage geometry are of particular importance, since they are likely to have the greatest influence on the propulsion system. The in-vacuo frequencies of the elastic modes are relatively low and closely spaced.

Propulsion Model

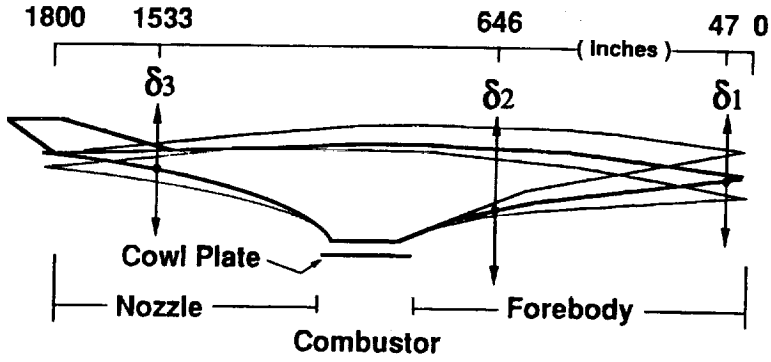

- Undersurface geometry analyzed by SRGULL
- Assumptions: 2-d forebody and nozzle
  1-d combustor
  no unsteady propulsion aerodynamics
- General form of model: $\begin{Bmatrix} F_A \\ F_N \\ M \end{Bmatrix} = f(\delta 1, \delta 2, \delta 3, \alpha)$

PROPULSION MODEL

The propulsion model was developed using the SRGULL code for hypersonic propulsion systems. The SRGULL code uses a two-dimensional inviscid Forebody and inlet analysis, and a one-dimensional combustor analysis to address the entire propulsion system flowpath shown in the figure. A variable grid is used to analyze the vehicle nose-to-tail stream tube control volume, determining mass capture, forebody and inlet drag, and combustor and nozzle performance. The nose-to-tail propulsion flowpath consists of the undersurface of the fuselage forebody, the combustor module, and the undersurface of the fuselage afterbody (serving as the nozzle). Using SRGULL, a database was produced which allows the interpolation of propulsive axial and normal force and pitching moment perturbations resulting from a given structural deflection at a given angle of attack.

To produce the propulsive force and moment database, the SRGULL code was first run at both flight conditions (Mach 6 and Mach 10) for the undeflected vehicle geometry over an angle-of-attack range from -1 to 3 degrees in one-degree increments. Structural deflections were then generated at selected stations along the fuselage centerline by calculating the RMS elastic responses to a Von Karman spectra turbulence input. Three stations along the fuselage centerline, designated as δ1, δ2, and δ3 in the figure were chosen to parameterize a set of perturbation geometries. The three stations are located 47 inches, 646 inches, and 1,533 inches back from the nose of the vehicle. The RMS deflections were then used to produce a collection of 27 perturbation geometries consisting of the set of all possible combinations of the upward, zero, and downward deflection positions at each of the three selected fuselage stations, assuming that the combustor section was rigid. Each of the perturbation geometries was then analyzed using SRGULL over the angle-of-attack range from -1 to 3 degrees at both Mach Numbers to produce a database of axial force, normal force, and pitching moment perturbations as a function of fuselage deflections and angle of attack. The data was then combined into a 4-dimensional interpolation table using angle of attack and the deflections at the three fuselage stations as the independent variables. Curve fits to the data were used to increase the number of breakpoints in the interpolation table. In this way, a database was produced which could be used to estimate the propulsive forces and moments for any deflected geometry by interpolating from the table based on angle of attack and the deflections at the three selected fuselage stations.

Propulsive Force and Moment Data

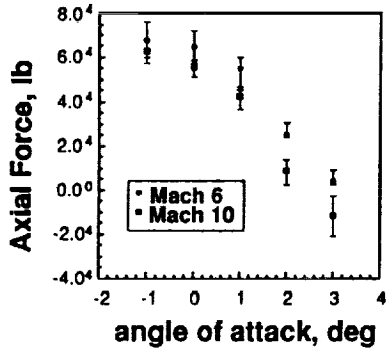

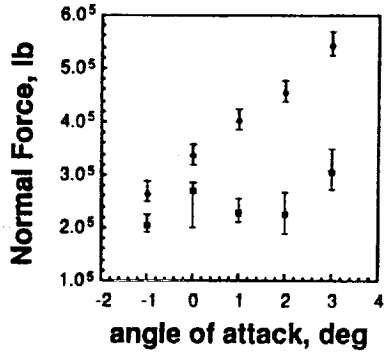

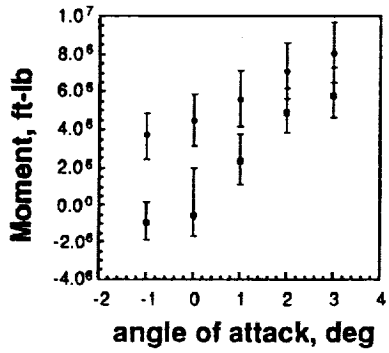

- **Large variation with alpha**
- **Symbols: data for undeflected geometry**
- **Brackets: range of variation due to perturbed geometries**

PROPULSIVE FORCE AND MOMENT DATA

The force and moment database produced using SRGULL is plotted against angle of attack in the figure. The solid symbols represent the data for the undeflected vehicle geometry at Mach Numbers of 6 and 10. The brackets about each symbol indicate the range of variation in axial force, normal force, or moment that resulted from the analysis of the 27 perturbation geometries.

Simulation Layout

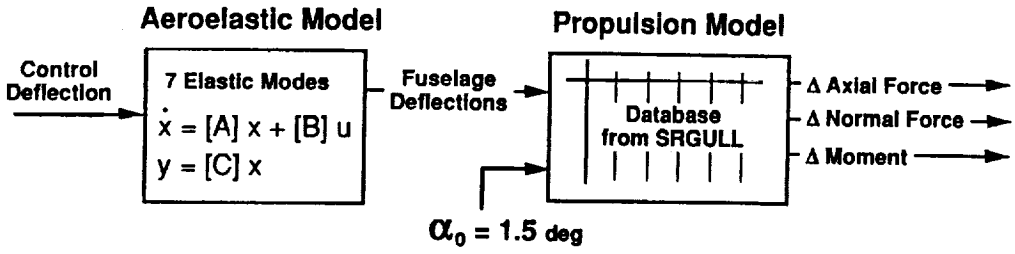

- **Removed rigid body modes from aeroelastic model**
- **Excited elastic modes with control doublet**
- **Examined magnitudes of elastically-induced propulsive perturbations**

SIMULATION LAYOUT

In order to ascertain the approximate magnitudes of elastic deflections and resulting propulsive perturbations which can be expected in response to a typical control input, a simulation was constructed incorporating the aeroelastic and propulsion models in the general structure shown in the figure. In this simulation, the aeroelastic model is driven by control surface deflections to yield an output vector, y, consisting of angle-of-attack perturbations and elastic deflections which are then fed into the propulsive interpolation database to produce time histories of the resulting force and moment perturbations. The rigid body dynamics of the aeroelastic model are unstable at both flight conditions and were removed so that these time histories could be produced in the absence of the divergent rigid body motion. The time histories were generated using the propulsive force and moment interpolation database at an angle of attack of 1.5 degrees. This angle of attack did not change during the time histories, since the angle-of-attack perturbations did not occur in the absence of the rigid body modes. Therefore, the propulsive perturbations produced by the control doublet are entirely the result of elastic fuselage deformations and not of angle-of-attack variations. Also, the perturbations do not include the aerodynamic lift, drag, or moment acting on the control surface itself. The responses do not represent worst case perturbations, but rather are intended to provide insight into the magnitude of the propulsion system sensitivity to elastic deformation of the vehicle.

Perturbation Time Histories

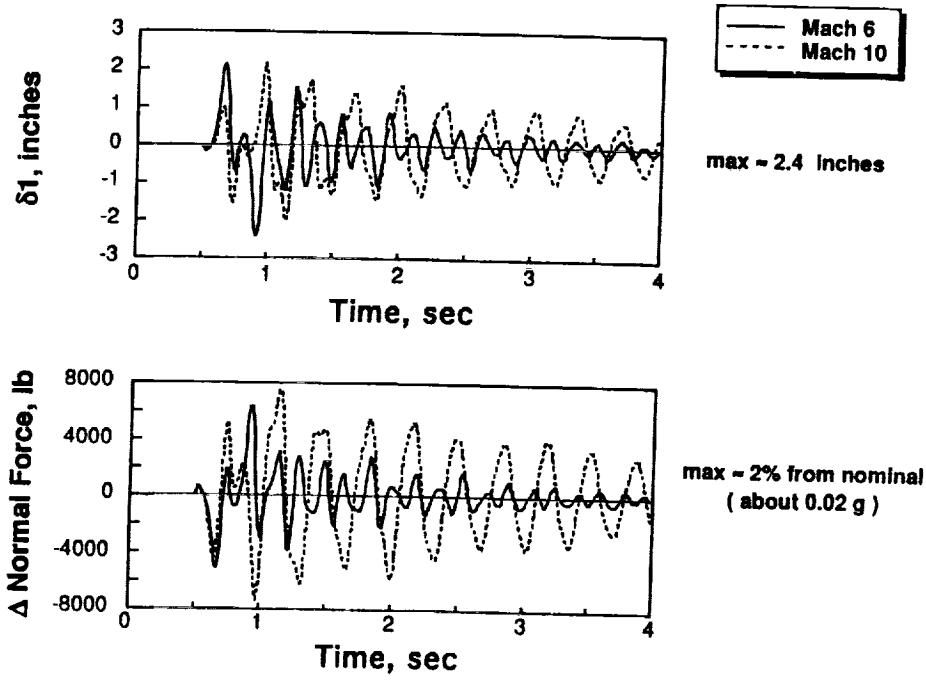

PERTURBATION TIME HISTORIES

Time histories of the elastic deflections at the first station along the fuselage centerline designated as δ1 (47 from the nose of the vehicle) are shown in the figure for the Mach 6 and Mach 10 flight conditions. The doublet was initiated 0.5 seconds into the run. The largest fuselage deflections reach about 2.4 inches at this fuselage station. These deflections appear to represent relatively minor distortions of the aerodynamic compression surface of the integrated airframe-propulsion system. The deflections did not produce appreciable accelerations at the pilot station.

Time histories of the propulsive force and moment perturbations resulting from the elastic deflections are also shown. The largest normal force perturbations range from 6,390 lbs for the Mach 6 case to 7,580 lbs for Mach 10 case.

Perturbation Time Histories

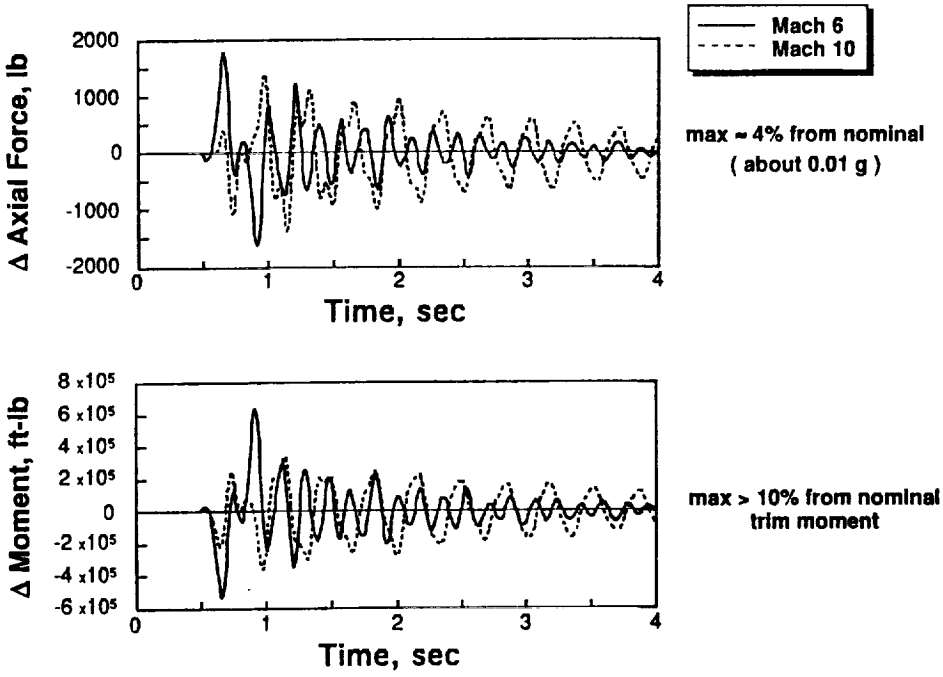

max ≈ 4% from nominal
(about 0.01 g)

max > 10% from nominal
trim moment

PERTURBATION TIME HISTORIES (continued)

The largest axial force perturbations range from 1,770 lbs to 1,410 lbs, and the pitching moment perturbations range from 6.32 x 10^5 ft-lbs to 3.60 x 10^5 ft-lbs in the Mach 6 and Mach 10 cases, respectively. The maximum normal force perturbations represent approximately 2 percent variations from nominal and would produce vertical acceleration transients of about 0.02 g's for a vehicle weighing 300,000 lb. The maximum axial force perturbations represent approximately 4 percent variations from nominal and would produce longitudinal acceleration transients of less than 0.01 g's for a vehicle weighing 300,000 lb. The maximum moment perturbations, however, represent greater than 10 percent variations from the nominal trim moment and may require substantial control deflections to maintain stable trimmed flight. It is important to remember that these force and moment perturbations are due solely to propulsion system sensitivity to elastic deflections. They do not include the effect of angle-of-attack perturbations on the propulsion model. The large pitching moment variation is due mainly to the aerodynamic contribution of the forebody. Maintaining trim in presence of the large pitching moment perturbations may require excessive control activity in hypersonic flight, which could translate into a substantial drag increment when integrated over the duration of a mission, implying reduced fuel efficiency and decreased payload capacity.

Simulation Layout

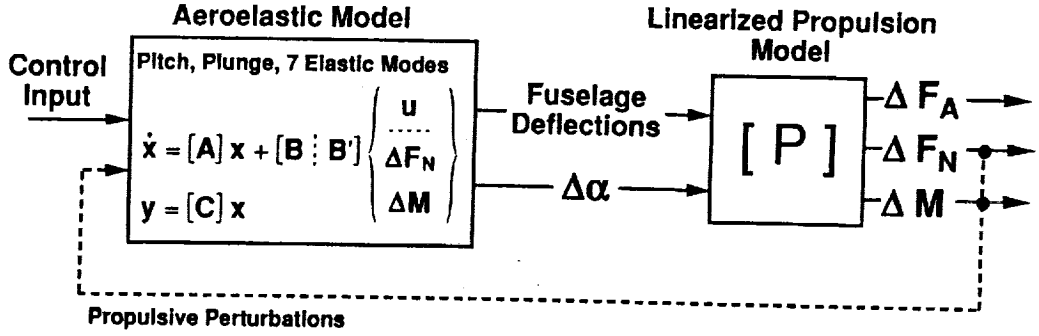

- **Examine impact of propulsive perturbations on aeroelastic model.**
- **Equates to augmenting the stability matrix:**

$$\dot{x} = [A]x + [B]u + [B'][P][C]x \text{ , or}$$

$$\dot{x} = [A + A']x + [B]u \quad \text{where} \quad A' = [B'][P][C]$$

- **Propulsive force and moment perturbations treated as "virtual inputs" applied at cg.**

SIMULATION LAYOUT

The simulation was used to assess the impact of the propulsive perturbations on the dynamics of the combined aeroelastic-propulsive system. This was accomplished by feeding the propulsive force and moment perturbations back into the aeroelastic model as indicated by the dashed line in the figure. As shown in the figure, this simply equates to augmenting the stability matrix with the effect of the linearized propulsion sensitivities. The model contains a further approximation in that the propulsive force and moment perturbations are applied at the cg, rather than being distributed over the aft nozzle area and cowl structure of the vehicle. Application of forces and moments to the aeroelastic model at the cg produces acceptable results regarding the impact of the propulsive perturbations on the vehicle's rigid body dynamics (pitch and plunge), but should not be used to assess the impact of propulsive perturbations on the elastic modes. In order to achieve the latter, it would be necessary to apply the propulsive perturbation loads to the structure using an appropriate load distribution function.

Impact on Rigid Body Modes

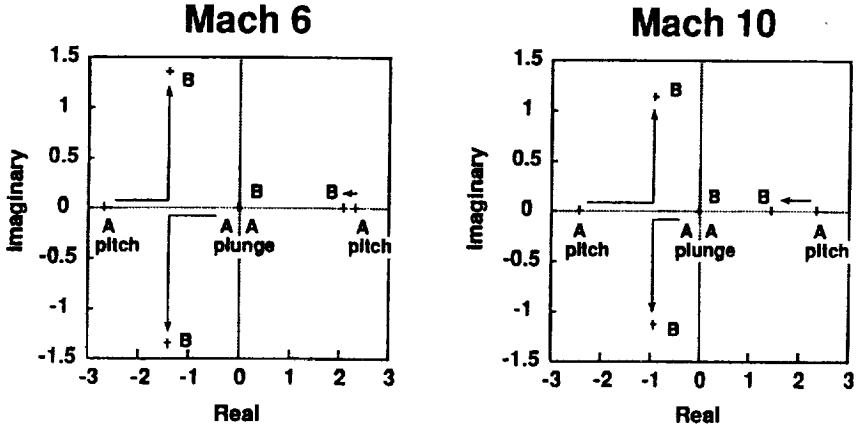

- Illustrates impact on rigid body modes due to augmenting stability matrix with propulsion system sensitivities.
- Propulsion linearization conditions: $\alpha_0 = 1.5$ deg, $\delta_0 = 0$
- Final position of eigenvalues was strongly dependent upon linearization conditions of propulsion model.

IMPACT ON RIGID BODY MODES

The figure illustrates the effect of the propulsive perturbations on the rigid body dynamics for the Mach 6 and Mach 10 flight conditions. The roots labeled "A" in the figure represent the statically unstable pitch and plunge modes when the propulsive perturbations are not being fed into the aeroelastic model. When the propulsive perturbations are fed into the aeroelastic model, two of the poles associated with the rigid body modes are observed to couple, producing a new oscillatory mode. The frequency of the unstable pole associated with the pitch mode is also observed to vary. The final position of the rigid body roots is indicated by the points labeled "B" in the figure. The Mach 10 case exhibits a slightly greater variation in the frequency of the unstable root of the pitch mode.

Eigenvalue Dispersion Caused by Varying Linearization Conditions

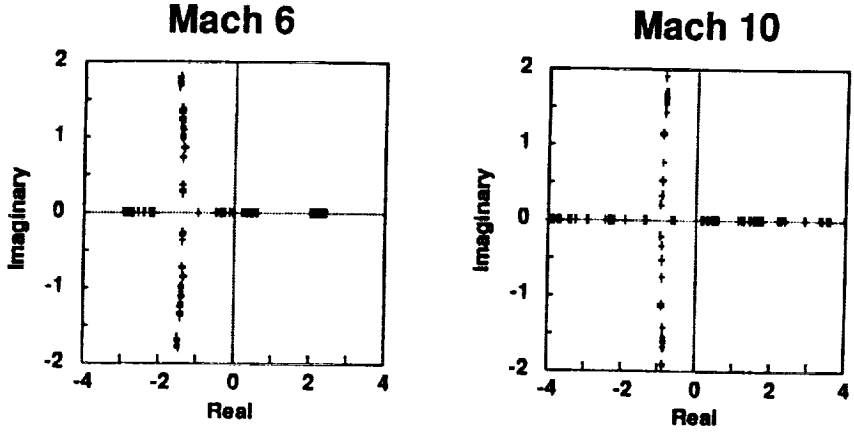

- Varied α_0 and δ_0 used to linearize propulsion sensitivities.
- Illustrates range of possible dynamic characteristics due to nonlinear propulsion database.
- Can be viewed as uncertainty associated with rigid body flight dynamics.

EIGENVALUE DISPERSIONS

It was found that the final position of the poles of the augmented stability matrix varied depending on the angle of attack and nominal fuselage deflections about which the propulsion model was linearized. This variation is a direct result of nonlinearities in the propulsive force and moment database. The nonlinearities introduce uncertainty into the system regarding the position of the rigid body poles, because the pole locations vary as the structure deforms and as angle of attack varies. In order to chart the pole variation resulting from nonlinearities in the propulsive force and moment database the propulsion linearization conditions were varied and corresponding eigenvalues of the augmented stability matrix were plotted. The angle of attack was varied over the range of -1 to 3 degrees, and nominal fuselage deflections were simultaneously varied according to the deflection time history shown in the previous figures. The resulting eigenvalue dispersions are shown in this figure. The variation of linearization conditions caused a wide range of dynamic characteristics to be observed at both flight conditions. This variation in dynamic characteristics due to the propulsion nonlinearities may be viewed as uncertainty associated with the rigid body modes.

Future Research

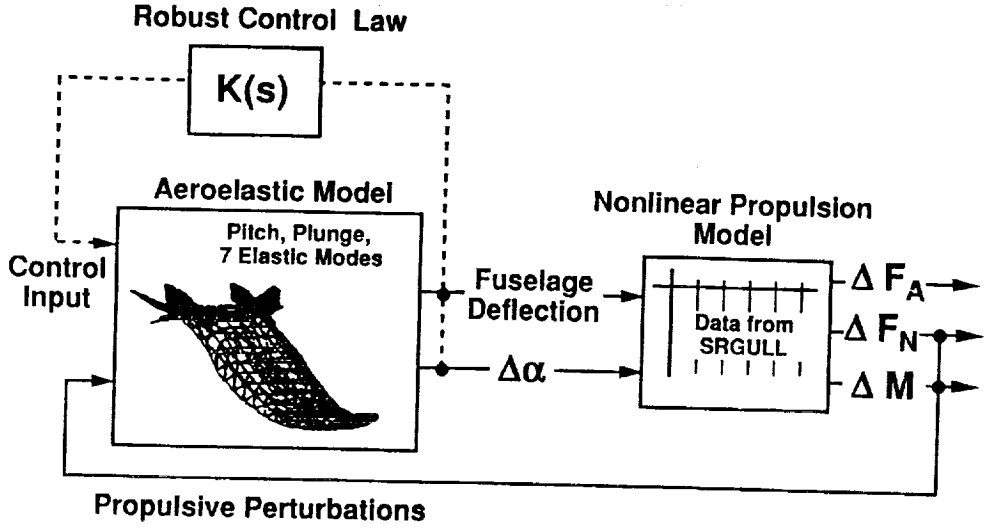

- Improve integration of aeroelastic/ propulsion models.
- Investigate control solutions for robust performance in the presence of ASPE interactions.

FUTURE WORK

Additional research is needed to refine the integration of the aeroelastic and propulsive models. Future work will also involve the formulation of uncertainty bounds on the various elements of the stability matrix resulting from the feedback of the propulsive perturbations into the aeroelastic model. These uncertainty bounds could then be used to synthesize a robust rigid body controller.

Concluding Remarks

- **Quantified propulsion sensitivities to angle-of-attack and fuselage elasticity.**
- **Elastically-induced propulsive perturbations did not cause excessive accelerations.**
- **Propulsive moment perturbations may require excessive control deflection to maintain stable trimmed flight.**
- **Propulsion sensitivities significantly alter rigid body flight dynamics.**
- **Nonlinearities in propulsion sensitivities may be viewed as uncertainty in rigid body dynamics.**

CONCLUDING REMARKS

A study has been conducted to investigate the impact of aeroelastic-propulsive interactions on the longitudinal flight dynamics of an air-breathing hypersonic vehicle. A model was developed based on a finite element representation of a hypersonic configuration at two flight conditions of Mach 6 and Mach 10. The model included rigid body pitch and plunge modes and seven elastic modes, as well as propulsion system sensitivities to angle-of-attack variations and structural deflections. The model was incorporated into a simulation to produce time histories of propulsion force and moment perturbations in response to elastic deflections. The force and moment perturbations were then fed back into the aeroelastic model to allow their impact on the dynamics of the combined aeroelastic-propulsive system to be assessed.

The propulsion model exhibited a pronounced sensitivity to angle-of-attack variations and elastic fuselage deflections. Significant nonlinearities were observed in the propulsion system sensitivities. Elastic responses to a representative control input appeared acceptable. The normal and axial force perturbations induced by the elastic deflections were appreciable, but did not produce excessive vertical or longitudinal acceleration transients for the subject configuration. Moment perturbations induced by the elastic deflections, however, appeared quite large and might require significant control activity to maintain stable trimmed flight. A high level of control activity at hypersonic speeds could compromise fuel efficiency, thereby reducing payload capacity or range.

A significant impact on the rigid body flight dynamics was observed when the propulsive force and moment perturbations were fed back into the aeroelastic model. At both flight conditions, the propulsive perturbations caused a coupling of two poles associated with the rigid body flight dynamics. It was also found that the eigenvalues of the rigid body modes were highly sensitive to the angle of attack and nominal fuselage deflections chosen as the linearization condition of the model. This sensitivity is a direct result of nonlinearities in the propulsive force and moment database, and can be thought of as uncertainty associated with the vehicle's rigid body stability coefficients. Considerable variation in the rigid body modes was observed, emphasizing robustness as a critical factor in the design of flight control laws for air-breathing hypersonic vehicles.

C-6.

Launch-Vehicle Trajectory Solutions with Dynamic-Pressure Constraints Via Finite Elements and Shooting

Robert R. Bless*, LESC

Hans Seywald*, AMA

Dewey H. Hodges, Georgia Tech

*Guidance Group, Spacecraft Controls Branch

NASA LaRC Workshop on Guidance, Navigation, Controls, and Dynamics for Atmospheric Flight

March 18 – 19

Outline

- Optimal Control Problem Definition
- State Constraints
- Methods of Solution
  - Multiple Shooting
  - Finite Elements
- Launch-Vehicle Model
- Results
- Summary

Problem Definition

$$\text{minimize} \quad J = \phi[x(t_f), t_f] + \int_0^{t_f} L(x, u, t)\, dt$$

subject to state equations $\dot{x} = f(x, u)$

boundary conditions $\psi[x(t_f), t_f] = 0$

control constraints $C(x, u, t) \leq 0$

and state constraints $S(x, t) \leq 0$

Result is a nonlinear multi-point boundary-value problem

State Constraints

Consider active state constraint for $t_1 \leq t \leq t_2$

$$S(x) = 0$$

is equivalent to

$$S[x(t_1)] = 0$$

$$\vdots$$

$$\frac{d^{(q-1)} S[x(t_1)]}{dt^{(q-1)}} = 0$$

and

$$\frac{d^q S}{dt^q} = S^{(q)}(x, u) = 0 \quad \text{for} \quad t_1 \leq t \leq t_2$$

Multiple Shooting Method

- Initial guesses chosen for states and costates
- Differential equations integrated forward
- Guesses updated via zero-finding method
- Process repeats until all boundary conditions are satisfied

Finite Element Method

- Discretization of continuous-time necessary conditions
- Set of nonlinear algebraic equations generated
- Initial guesses required for each element along trajectory
- Nonlinear equations can be solved by Newton-Raphson method

Comparison of Methods

- Shooting
  - Sensitive to initial guesses
  - Slow iteration process due to integration
  - Numerically exact answer is found
- Finite Element
  - Initial guesses more easily obtained
  - Fast iteration process (sparse Jacobian)
  - Second-order accuracy

Finite element solutions can provide guesses for shooting

Launch-Vehicle Model

- NLS two-stage rocket (point-mass model)
  - States are mass, altitude, velocity, and flight-path angle
  - Scalar control is angle-of-attack
  - Fixed staging time; change in thrust and mass
  - Exponential atmosphere
  - Piecewise constant aerodynamic coefficients

Launch-Vehicle Model (continued)

- Mission
  - Maximize final mass
  - Perigee injection of 80 $\times$ 150 NM orbit
- Constraint on maximum dynamic pressure
- Engine out on pad

Results

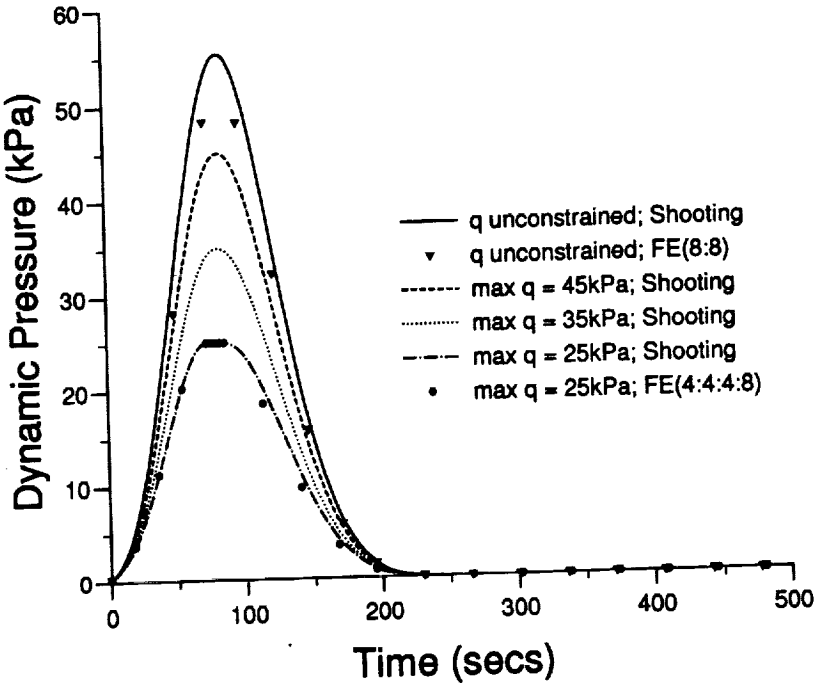

Results

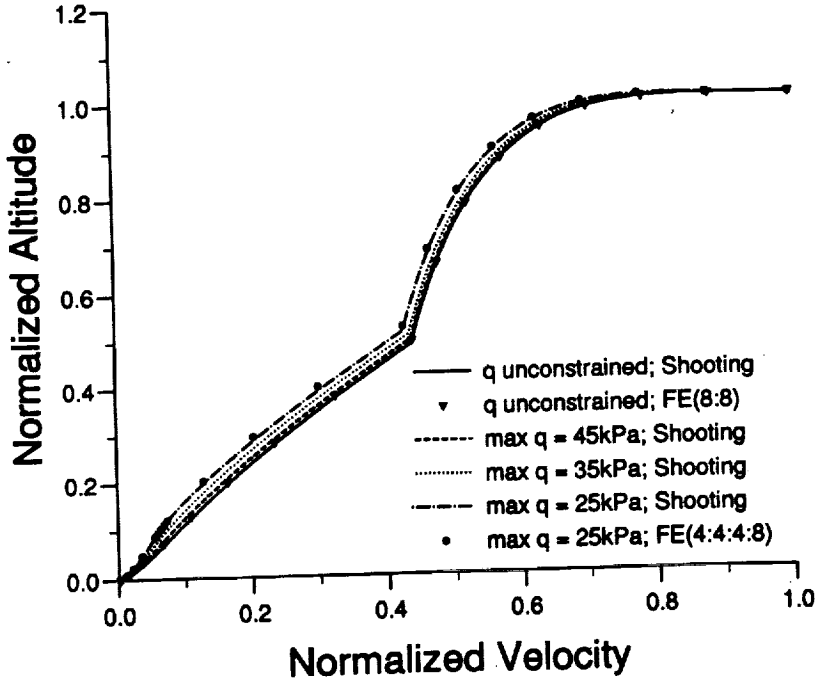

Results

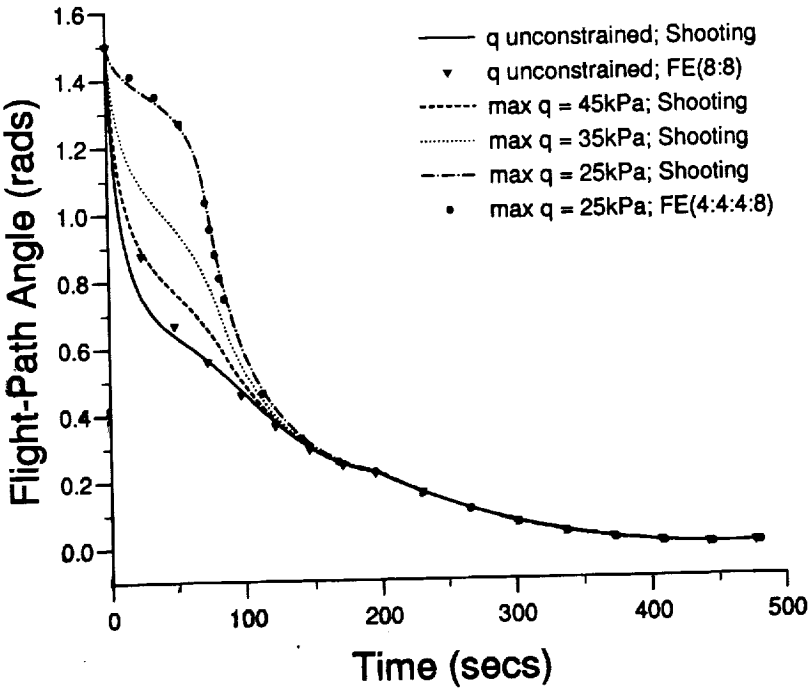

Results

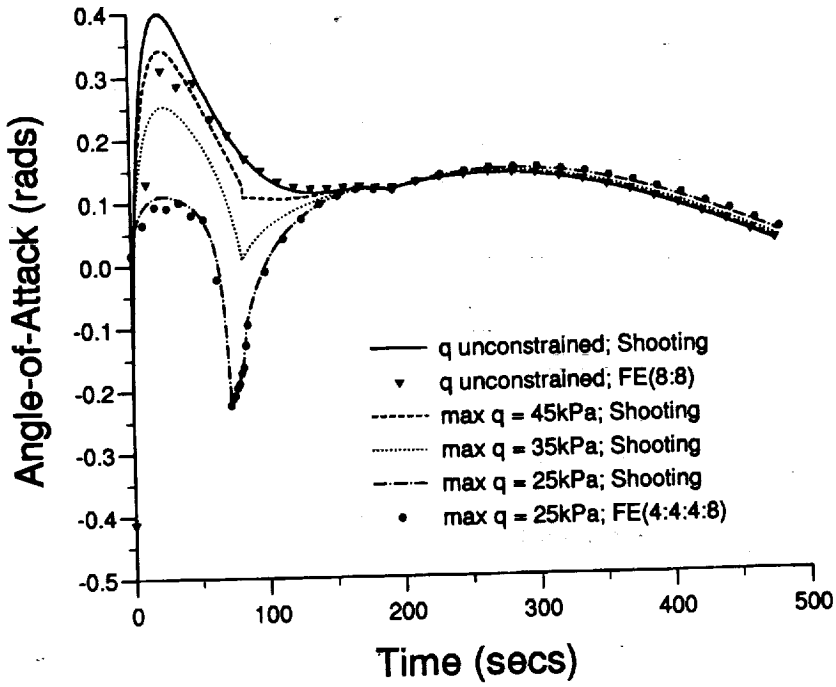

Results

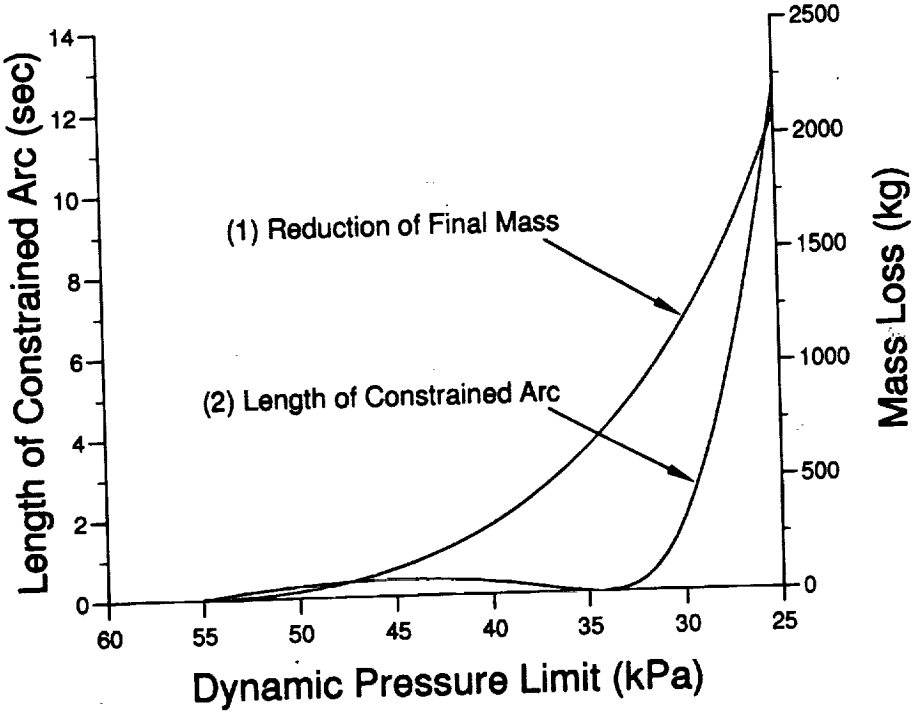

Summary

(1) The finite element and shooting methods are complementary algorithms

(2) The work has produced a family of dynamic-pressure constrained solutions

(3) An uncommon first-order touch-point solution has occurred (not observed in literature yet)

(4) This work will be reported on at the AIAA GNC Conference in August

  (a) Derivation of finite element method

  (b) Discuss touch-point behavior